

# Film Composite of Carrageenan with Carbon Nanodots: Preparation, Characterization, and Investigation on Heavy Metal Sensing

Jessa Leuterio<sup>1</sup>, and Drexel Camacho<sup>1, 2\*</sup>

<sup>1</sup> *Chemistry Department, De La Salle University, 2401 Taft Avenue, Manila, Philippines*

<sup>2</sup> *Central Instrumentation Facility, De La Salle University Laguna Campus, LTI Spine Road, Biñan, Laguna*

*\*Corresponding Author: drexel.camacho@dlsu.edu.ph*

**Abstract:** Carbon nanodots (CNDs) are excellent nanomaterials that received significant interest lately because it exhibits unique high-fluorescence properties. This study investigates the potential of  $\gamma$ -carrageenan as a carbon source for CNDs. Hydrothermal process afforded CNDs that exhibited fluorescence property under UV light. The CNDs were embedded in the carrageenan film to prevent its aggregation and to increase its stability for further applications. The CNDs embedded in films show different properties compared to bare CNDs in solution as determined by Dynamic Light Scattering, Zeta potential, UV-Vis, Fluorescence, and FTIR spectroscopies. The films loaded with CNDs were explored for its application in sensing heavy metals. Results showed the potential of CNDs in films to selectively detect  $\text{Cu}^{2+}$  using digital colorimetric analysis.

**Key Words:** Carbon nanodots, Carrageenan, Film composite, Sensing, Heavy metal

## 1. INTRODUCTION

Carbon nanodots (CNDs), also referred to as fluorescent carbon, are a new kind of carbon nanomaterial with sizes below 10 nm that exhibit strong fluorescence property. They have high solubility in water, high stability under light, low toxicity, and can be modified chemically. Applications using CNDs have been developed into exciting materials (Baker & Baker, 2010). The preparation of CNDs can be done from bulk materials but requires expensive equipment, exposures to harsh chemicals, and usage of toxic reagents. Another approach involves assembling atoms from degraded organic compounds such as carbohydrates to form CNDs, which was done under heating, ultrasounds, or microwave conditions (Roy et.al, 2015). Hydrothermal method is another technique that uses water with the organic precursor in a sealed container heated at above the boiling point of water. The high pressure

inside degrades the precursor without releasing  $\text{CO}_2$  and allows the assembly of carbon atoms to form CNDs. The technique is simple and is an eco-friendly way of transforming available materials into useful products. Biomasses such as onion, lemon peel, ginger and egg white have been converted into CNDs using hydrothermal method (Kang et al., 2020).

Carrageenan, a sulfated polysaccharide from red seaweeds, is a biomolecule used in food industry owing to its gelling, thickening, and emulsifying properties. The Philippines is a major supplier of carrageenan worldwide. This work explores non-food applications of carrageenan to add value products that would benefit the seaweed farmers and the carrageenan industry. The three major types of carrageenan are kappa, iota, and lambda, which vary from one another by the amount and position of ester sulfate groups in their galactose dimer. This work explored the utilization of  $\gamma$ -carrageenan as starting material for the synthesis of CNDs. The utilization of sulfate-containing polysaccharides to prepare CNDs

are interesting because this functional group may play an important role in activities such as heavy metal sensing. Moreover, the work investigates the possibility of stabilizing the CNDs by keeping them separate in a film matrix.

## 2. METHODOLOGY

### 2.1 Materials

Food grade  $\nu$ -carrageenan was obtained from Mioka biosystems. Teflon-coated stainless autoclave was used for the hydrothermal method. PVDF syringe filter (Whatman, 0.2 $\mu$ m) was used to purify the CNDs. Freeze dryer (Christ Gamma 2-16 LSCPlus) was used to dry CNDs. The following instruments were used to characterize the CNDs: UV-vis (Shimadzu UV-2600), SEM (JEOL SM-IT500HR) equipped with EDX, Fluorescence Spectrophotometer (Shimadzu RF-6000), FTIR (Agilent Cary 630), and Dynamic Light Scattering (Malvern, Nano-ZSP Zetasizer).

### 2.2 Preparation of carbon nanodots (CNDs)

CNDs were prepared by dispersing the iota-carrageenan (2.0 grams) in 40 ml distilled water stirred continuously for 15 minutes. The mixture was agitated in an ultrasonicator bath for 20 minutes and transferred to a Teflon-lined stainless autoclave (100 ml). The sealed autoclave was placed in a drying oven at 200°C for 4 hours. The mixture was cooled to room temperature and was subjected to centrifugation at 15,000 rpm for 20 minutes to separate the black solid particle (hydrochar) from the mixture. The obtained yellowish-brown solution was collected and purified using PVDF syringe filter. The CNDs were collected and freeze-dried. A solution of CND was made by redispersing the CND in deionized (DI) water.

### 2.3 Preparation of film composite with CNDs

The raw CND solution (10 ml) was mixed thoroughly with 1% wt/v  $\kappa$ -carrageenan (100 ml) and was heated at 45°C for 15 minutes. Fixed volume (35 ml) of the mixture was deposited evenly in a plastic polypropylene petri dishes to achieve a uniform film thickness. The mixture was cooled until it formed a gel, then allowed to dry at room temperature to give a thin film. The films were cut into square (2" x 2") size.

### 2.4 Characterization of CNDs in solution and in film

The UV-vis absorption spectra of the raw

CND solutions and CND films dissolved in DI water were measured at wavelength scan from 200 to 700 nm. The fluorescence spectra were recorded at excitation wavelength from 320 nm to 440 nm in 20 nm increments and emission wavelength from 300 nm to 800 nm at RT in aqueous solutions. Hydrodynamic size and zeta potential were measured using Dynamic Light Scattering (DLS). The surface charge and size distribution of CNDs were determined by Zeta-sizer. The morphology and elemental analysis of freeze-dried CNDs were determined using SEM with EDX. The FTIR spectra of the freeze-dried CNDs and the CND films were obtained using FTIR-ATR in the range of 4000-400  $\text{cm}^{-1}$  accumulating 64 scans at RT.

### 2.5 Investigation on the effects of CND films in heavy metals

The detection of metal ions was examined using the fluorescence properties of the film-based CNDs in the presence of various metal ions (Ni (II), Cu (II), Pb (II), Cr (VI), Cd (II) and Hg (II)). The film-based CND from  $\nu$ -carrageenan, cut in 2" x 2" size, was dissolved in 200 ppm solution of the metal ions for 20 mins for color development and stabilization. The images of the metal solutions with dissolved film-based CNDs were captured under UV light by Nikon D3200 DSLR camera with ISO automatic, auto white balance, no flash, and macro settings.

## 3. RESULTS AND DISCUSSION

The food-grade  $\nu$ -carrageenan precursor when dispersed in water formed yellow colloidal mixture but upon hydrothermal carbonization at 200°C for 4 hours, the mixture changed to yellowish-brown accompanied by a noticeable formation of black particles called the hydrochar (Fig 1). The separation of the supernatant from the hydrochar through high-speed centrifugation and syringe filtration afforded the CNDs in aqueous dispersion. The resulting CNDs were freeze-dried to afford sticky black powders, which can be redispersed in water. The redispersed CNDs afforded a brownish yellow color under daylight but turns luminous green under UV light. Incorporation of the CNDs into  $\kappa$ -carrageenan film yielded a stable brownish yellow film, which again turns luminous green under UV light. The incorporation of the CNDs in the film is envisioned to provide long term stability of the CNDs by keeping them separate in the film matrix prior use in various applications. Storing CNDs in solution will result to aggregation over time, which then eliminates its nano

dimension and unique properties.

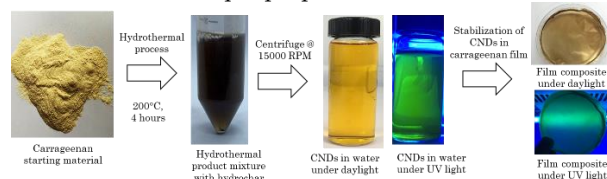


Fig. 1. Preparation of CNDs

SEM and TEM images of the freeze-dried  $\nu$ -carr-CNDs were attempted but showed non-separated particles as it was very hygroscopic forming a paste. Nevertheless, a quasi-spherical shape can be observed in SEM (Fig 2A), which is characteristic of CNDs. Due to the difficulty in measuring the size of the CNDs, hydrodynamic size was measured in the presence of water as solvent using Dynamic Light Scattering (DLS). Results showed that the average hydrodynamic size of  $\nu$ -carr-CNDs, is  $2.3 \pm 1.62$  nm (Fig 4A). EDS spectrum (Fig. 2B) confirmed the elements present in CNDs from carrageenan precursors. The result showed that the CNDs from  $\nu$ -carrageenan were composed of C ( $52.79 \pm 0.40\%$ ), O ( $39.01 \pm 0.67\%$ ), S ( $4.19 \pm 0.19\%$ ), K ( $2.26 \pm 0.20$ ), Na ( $1.20 \pm 0.10$ ), and Mg ( $0.55 \pm 0.07\%$ ). Majority is made of carbon followed by oxygens that may have been formed in the periphery of the CNDs as oxides, carboxylates, or hydroxides. The metal cations are present in raw carrageenans as they naturally interact with the sulfate ester groups of carrageenan. These cations are responsible for the natural gelling characteristics of carrageenan as it forms complexes trapping the water molecules inside. This indicates that the elements present in the precursor was retained upon the conversion of carrageenan to CNDs.

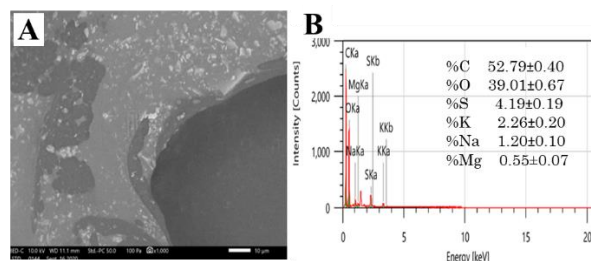


Fig. 2. (A) SEM image of CNDs, (B) EDS spectrum of the freeze-dried CNDs

The result was confirmed in FTIR analysis where the characteristic peaks of the starting materials are retained in the CNDs. The CNDs showed peaks at  $3300\text{ cm}^{-1}$  (hydroxide band),  $2900\text{ cm}^{-1}$  (C-H stretching),  $1022\text{ cm}^{-1}$  (C-O stretching), and  $1189\text{ cm}^{-1}$  (O=S=O symmetric vibration).

The raw CNDs exhibited two optical absorbance peaks in the UV region at around 200-300 nm (Figure 3A) attributed to the  $\pi$ - $\pi^*$  transition peak due to  $\pi$  conjugated aromatic system and the highest absorbance peak ( $\lambda_{\text{max}}$ ) observed at 282 nm was attributed to the  $n$ - $\pi^*$  transition of the carbonyl and other oxygen-containing compounds that is very prevalent in carbon nanodots (Wu et al., 2015). This result indicates that  $\nu$ -carrageenan was completely transformed into CNDs thru the hydrothermal process. The effect of the carrageenan film matrix on the absorbance spectra of the CNDs was observed by dissolving the composite films in water. The two absorbance peaks around 200-300 nm are still visible attributed to the CNDs. However, a shift of  $\lambda_{\text{max}}$  absorbance to a shorter wavelength (251 nm) was observed (Fig 3C) indicating that the polymer matrix has an effect on the absorbance of CNDs. The observed blue shift can be attributed to the interaction between the carbonyl groups of CNDs and carrageenan which affects the  $n$ - $\pi^*$  transition peaks of the  $\pi$  conjugated aromatic system of CNDs. Spectrofluorometric analysis was conducted to study the fluorescence characteristics of the CNDs in an aqueous medium. The emission spectrum of  $\nu$ -carr-CNDs proved the excitation-dependent emission feature of CNDs. By employing increased excitation wavelength from 320 to 420 nm. A red shift was observed as the excitation wavelengths increases, followed by the decrease of the fluorescence intensity (Fig 3B). The shift in emission peak with changing excitation energy is noticeable in the emission spectrum, which showed strong emission peak centered at 435 when excited at 340 nm indicating that the raw CNDs are fluorescent in nature. To observe the effect of the carrageenan film matrix in the fluorescence property of CNDs, the composite film was dissolved in water and the emission spectra showed a prominent peak at the onset of the scan, which was only observed as a shoulder peak in raw CND. Notably, the fluorescence intensity in the case of film-based CNDs decreases

compared to in CND solutions due to the decrease in CND concentration. Still a red shift was noticed as the excitation wavelengths increases, followed by the decrease of the fluorescence intensity where it showed a strong emission peak centered at 400 nm when excited at 320 nm. The red shift in the emission spectra may be associated to the inhomogeneous size distribution of CNDs along with the presence of different surface states created by numerous functional groups such as C-O, C=O and O=C-OH (Mehta et al., 2015). When CNDs are excited by a photon of a specific wavelength, these surface traps prevail but when they are excited with a different wavelengths, other types of emission traps dominate. This results to the  $\lambda_{ex}$  dependence of CNDs. The difference of the intensity in maximum fluorescence was due to decrease in concentration of CNDs. Diluting CNDs in deionized water lessens collision extinguishment and self-absorption in high concentrations.

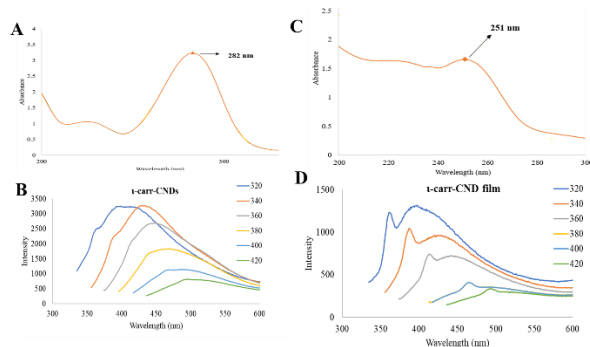


Fig. 3. Raw CNDs in water: (A) UV spectrum, (B) Emission spectra. CND composite film dissolved in water: (C) UV spectrum, (D) Emission spectra

Investigation on the hydrodynamic size of the CNDs using DLS requires dispersion in water. Despite the interaction with solvent molecules, the raw CNDs afforded a small hydrodynamic size reading ( $2.3 \pm 1.62$  nm) (Fig 4A). The effect of the film matrix on the hydrodynamic size of CNDs was determined by dissolving the CND-film in water. The measured hydrodynamic diameter of the CNDs from the CND-films was found to be  $261 \pm 207.4$  nm (Fig 4B). The effect of the presence of  $\kappa$ -carrageenan in the film matrix causes to increase the measured hydrodynamic CND sizes in the film-based CNDs. The

surface of CNDs interacts not only with the water solvent but also with the polymeric film matrix dissolved in water. A strong hydration occurred between the electrical charges on the CND surface with the  $\kappa$ -carrageenan since it is highly negatively charged due to the sulfate groups attached in it. This leads to a great charge density all over the surface of CNDs.

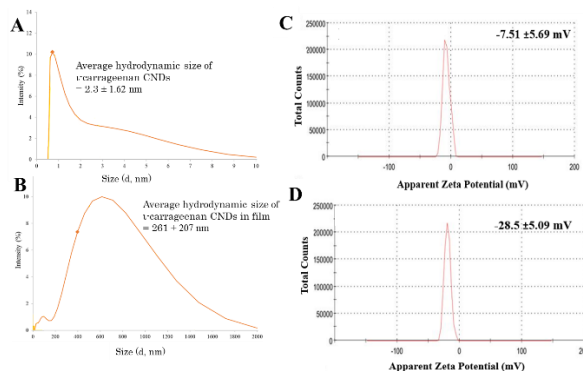


Fig. 4. (A) Hydrodynamic size of the raw CNDs in aqueous solutions, (B) Hydrodynamic sizes of the CNDs in the composite films, (C) Zeta potential of the raw CNDs in water, (D) Zeta potential of the CNDs in composite films.

The zeta potential measurement of CNDs (Fig 4C) showed that the  $\kappa$ -carr-CNDs has negative surface potential with high charge densities ( $-7.51 \pm 5.69$  mV) indicative of the presence of a negative functional groups on CNDs, which can be attributed to the carboxyl, hydroxyl, and the sulfate groups present in CNDs. The effect of the film matrix in the zeta potential of CNDs was also determined by dissolving the CND composite film in water. The  $\kappa$ -carr-CND film afforded more negative surface potentials ( $-28.5 \pm 5.09$ ) compared to the CNDs in solution (Fig 4D). A high value of positive or negative zeta potential of a particle shows good physical stability of nano-suspensions due to electrostatic repulsion of individual particles. A value greater than  $+30$  mV to  $-30$  mV is generally considered to have enough repulsive force to achieve better colloidal stability, while a small zeta potential value can result in particle aggregation and flocculation due to the van der Waals attractive forces enforced upon them in which may result in physical instability (Joseph &

Singhvi, 2019). The change from  $-7.51 \pm 5.69$  to  $-28.5 \pm 5.09$  zeta potential value of  $\iota$ -carr-CNDs indicated that the film matrix causes it to attain better colloidal stability. Since  $\kappa$ -carrageenan film matrix contains high content of sulfate groups, this leads to a greater charge density all over the surface of CNDs causing it to increase to a more negative zeta potential value.

In this work, the possible use of CNDs as a fluorescent probe was explored based on their fluorescence intensity color for the potential detection of heavy metals. Although heavy metals are crucial for life and the environment, they are toxic to living organisms at certain concentrations, so the detection of heavy metals using cheap materials for point-of-use application is necessary. Without the need for specialized instruments such as AAS, ICP, etc. and the need to do tedious wet processing of the samples for metal detection, it is highly desired to develop a material that detects the presence or the absence of the heavy metals in polluted water. A handy material that can be used on-field, by dissolving the film containing the fluorescent CNDs in water loaded with heavy metal is described. Since it fluoresces, the study surmises that the interaction of the CNDs with the metals might produce a complex that could change in color thereby sensing the metal. The CND-loaded composite film, which remains stable over time was used as a sensor by dissolving it in water that contains heavy metal ions. The images of  $\iota$ -carr-CND films dissolved in different metal solutions (200 ppm of  $\text{Cu}^{2+}$ ,  $\text{Ni}^{2+}$ ,  $\text{Pd}^{2+}$ ,  $\text{Hg}^{2+}$ ,  $\text{Cd}^{2+}$ ,  $\text{Cr}^{6+}$ ) under UV light were analyzed using RGB analysis of Color Image software and obtained RGB values were converted to CIEL\*a\*b\* values using Easy RGB free online color converter software (<https://www.easyrgb.com/en/convert.php>). Figure 5 showed the absorbance response of  $\iota$ -carr-CND film in the presence of different metal ions. It was shown that among the metals tested, the most responsive metal is the  $\text{Cu}^{2+}$  showing an observable decrease in absorbance peak at 283 nm while other ions had slight or no interference to absorbance. The screening indicates the potential  $\iota$ -carr-CND film to show slight selectivity for  $\text{Cu}^{2+}$ .

In this work, the fluorescence color of CNDs showed a green color under UV light. Thus, for the colorimetric detection on the change in color the

parameter that was observed is the green value in the digital analysis. The digital image parameters of the

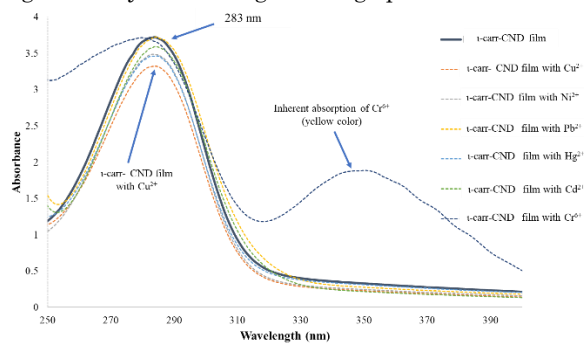


Fig 5. UV spectra of  $\iota$ -carr-CND film in the presence of different metal ions in aqueous solution

$\iota$ -carr-CND film dissolved in solution containing the different metal ions showed that the RGB values of the  $\iota$ -carr-CND film with metal ions exhibit a notable change from that of the  $\iota$ -carr-CND film dissolved in water. The digital image of the  $\iota$ -carr-CND film solution has the highest G value (104) verifying its distinct green color among the other metal solutions. The mixture with the lowest G value was observed in the presence of  $\text{Cu}^{2+}$  solution producing a G value of 70 (Table 1), which is a notable decrease from the G value 104 of the sensing mixture without the metal. This indicates that the green intensity color of  $\iota$ -carr-CND lowers in the presence of  $\text{Cu}^{2+}$ . The decrease of the color intensity of  $\iota$ -carr-CND under UV light was attributed to the fluorescence quenching happened between  $\text{Cu}^{2+}$ . The digital images of  $\iota$ -carr-CND film in different metal ions were likewise investigated in terms of the color space CIE parameters namely the  $L^*$  (lightness),  $a^*$  (green/magenta), and  $b^*$  (blue/yellow) in the chromatic axes. Lightness is measured from 0 (black) to 100 (white) thus, the high  $L^*$  value of the  $\iota$ -carr-CND film in solution confirms its intense bright appearance compared to the  $\iota$ -carr-CND film solution in the presence of metal cations. In the presence of  $\text{Cu}^{2+}$  ions, the  $a^*$  and the  $B^*$  values are notably different compared to the other metals. The results confirm the UV observation and the G values in the potential selectivity of the CNDs in sensing  $\text{Cu}^{2+}$  (Table 1). The results are attributed to the following possible reasons: (1) since  $\text{Cu}^{2+}$  is a soft acid while sulfur is a soft base, there is high affinity between  $\text{Cu}^{2+}$  and the sulfur moieties in  $\iota$ -carr-CNDs. This attraction affected the electron transfer on the surface of  $\iota$ -carr-CNDs, and increased the probability of non-radiative electron transition, which leads to fluorescence quenching. On the other hand, (2)  $\text{Cu}^{2+}$

forms a complexation with carboxyl groups and hydroxyl groups on the surface of  $\iota$ -carr-CNDs and increase the non-radiative transition of electrons and reduce the fluorescence intensity. The investigation showed the potential of CNDs from carrageenans for the selective sensing of  $\text{Cu}^{2+}$ . However, the result was not very observable in the naked eye limiting its use to the digital analysis. In the literature, the metal sensing ( $\text{Cu}^{2+}$  and  $\text{Hg}^{2+}$ ) capabilities of CNDs were enhanced if the CNDs were doped with nitrogen (Patir & Gogoi 2019) enhancing the complexation of the metal ions with the lone pairs of nitrogen present in the CNDs resulting to observable intense fluorescence. Another approach to enhance the sensing capabilities of CNDs was the incorporation of lanthanide ions and CNDs into a network of polyacrylamide and poly(acrylic acid) (Zhu et al. 2018).

Table 1. Digital analysis parameters of  $\iota$ -carr-CND film in different metal ion solutions

Color parameters	$\iota$ -carr-CND film	$\iota$ -carr-CND film with					
		$\text{Cu}^{2+}$	$\text{Ni}^{2+}$	$\text{Pb}^{2+}$	$\text{Hg}^{2+}$	$\text{Cd}^{2+}$	$\text{Cr}^{6+}$
R	40	30	28	29	32	26	42
G	104	70	73	91	80	81	77
B	113	123	166	92	121	104	25
$L^*$	40.481	29.628	30.089	35.034	32.754	32.041	29.082
$a^*$	-17.214	5.673	0.565	-18.931	-1.421	-9.479	-23.589
$b^*$	-11.118	-34.215	-29.096	-6.387	-28.005	-18.49	26.282

#### 4. CONCLUSIONS

Carbon nanodots were prepared from  $\iota$ -carrageenan using hydrothermal carbonization. The CNDs were embedded in a carrageenan film matrix allowing for the stabilization of CNDs and preventing aggregation. Properties of the CNDs in the presence of the film matrix showed different properties as compared to the bare CNDs in aqueous solution. Hydrodynamic size of CNDs was affected by the presence of polymer matrix but the polymeric carrageenan matrix afforded stability to the CNDs as shown by the observed Zeta potential. UV-Vis and fluorescence analysis confirmed the light absorbing properties of the CNDs. The film loaded with CNDs was found to sense the  $\text{Cu}^{2+}$  ions selectively and the detection can be observed using digital colorimetry.

Further studies are recommended to enhance the heavy metal sensing that are visible to the naked eye.

#### 5. ACKNOWLEDGMENTS

Jessa Leuterio acknowledges the DOST-SEI-ASTHRD for the scholarship and the DLSU – Central Instrumentation Facility (CIF) for the Graduate Thesis Residency Program.

#### 6. REFERENCES

- Baker, S. N., & Baker, G. A. (2010). Luminescent Carbon Nanodots: Emergent Nanolights. *Angewandte Chemie International Edition*, 6726–6744.
- Kang, C., Huang, Y., Yang, H., Yan, X.F., Chen, C.P. (2020). A Review of Carbon Dots Produced from Biomass Wastes. *Nanomaterials*, 10, 2316.
- Joseph, E., & Singhvi, G. (2019). Multifunctional nanocrystals for cancer therapy: A potential nanocarrier. *Nanomaterials for Drug Delivery and Therapy*. Elsevier Inc.
- Mehta, V. N., Jha, S., Basu, H., Singhal, R. K., & Kailasa, S. K. (2015). One-step hydrothermal approach to fabricate carbon dots from apple juice for imaging of mycobacterium and fungal cells. *Sensors and Actuators, B: Chemical*, 213, 434–443.
- Roy, P., Chen, P. C., Periasamy, A. P., Chen, Y. N., & Chang, H. T. (2015). Photoluminescent carbon nanodots: Synthesis, physicochemical properties and analytical applications. *Materials Today*, 18(8), 447–458.
- Patir, K., & Gogoi, S. K. (2019). Nitrogen-doped carbon dots as fluorescence ON-OFF-ON sensor for parallel detection of copper(ii) and mercury(ii) ions in solutions as well as in filter paper-based microfluidic device. *Nanoscale Advances*, 1(2), 592–601.
- Wu, Q., Li, W., Tan, J., Wu, Y., & Liu, S. (2015). Hydrothermal carbonization of carboxymethylcellulose: One-pot preparation of conductive carbon microspheres and water-soluble fluorescent carbon nanodots. *Chemical Engineering Journal*, 266, 112–120.
- Zhu, Q., Zhang, L., Van Vliet, K., Miserez, A., & Holten-Andersen, N. (2018). White Light-Emitting Multistimuli-Responsive Hydrogels with Lanthanides and Carbon Dots. *ACS Applied Materials and Interfaces*, 10(12), 10409–10418.